Ignition of DME and DME/CH₄ at High Pressure: Flow Reactor Experiments and Kinetic Modeling

H. Hashemi, J. M. Christensen, P. Glarborg*

DTU Chemical Engineering, Technical University of Denmark, DK-2800 Lyngby, Denmark

Abstract

The pyrolysis and oxidation of dimethyl ether (DME) and its mixtures with methane were investigated at high pressures (50 and 100 bar) and intermediate temperatures (450–900 K) in a laminar flow reactor. DME pyrolysis started at 825 K (at 50 bar). The onset of DME reaction was detected at 525−550 K (at 50 bar), independent of stoichiometry. The negative temperature coefficient (NTC) zone in the DME profile always included temperatures of 575−625 K. A profound promoting effect of DME addition on the ignition of methane was observed as the onset of reaction was shifted to lower temperatures by 50–150 K (at 100 bar).

Introduction

Combustion will remain the major source of energy for decades [1, 2]. The steady increase in the global energy demand as well as the release of carbon dioxide and harmful pollutants from the combustion of most fossil fuels are the major motivations to seek alternative sources of energy. In medium term, fossil-derived fuels which give rise to less pollutants and have a higher energy efficiency may relieve the environmental problems to some extent. Among the alternative fuels, dimethyl ether (DME) has attracted interest, especially for engines. DME can be produced from different feedstocks, e.g. oil, natural gas, coal, waste products, and biomass. Bio-derived DME fuel can potentially reduce the release of CO_2 to the environment. Lower ignition temperature, shorter ignition delay time, and easier evaporation compared to conventional diesel fuels make DME an attractive alternative. Replacing diesel fuel by DME reduces the emission of particulate matter (PM) and nitrogen oxides (NOx) from slightly modified compression-ignition (CI) engines [3–7]. The absence of a C−C bond in the molecular structure of DME, as well as its high oxygen content, are believed to suppress soot formation [4]. Using DME fuel in gas turbines has also been demonstrated and DME could replace natural gas in slightly modified gas turbines [8]. However, low energy density and potentially high emission of aldehydes and CO may challenge widespread usage of DME as a fuel [4].

DME has also been considered as an additive to improve combustion properties of various fuels, e.g. natural gas. Adding DME to natural gas accelerates ignition [9–12] and its addition to methane increases flame speed [10, 13]. Whereas DME accelerates methane ignition, its effect on ethane oxidation is more complicated [14]. Therefore it is vital to understand interactions between DME and the components of natural gas, especially since local variations in the composition of natural gas can be noticeable.

DME ignition and oxidation show a complicated behavior of negative temperature coefficient (NTC) at intermediate temperatures [15–18]. Ignition in engines and many industrial processes is strongly affected by combustion chemistry at high pressure and intermediate temperature. Despite this fact, DME oxidation has rarely been investigated at this range of temperature and pressure. Shock-tube measurements of ignition delay times by Pfahl et al. [15] at pressures up to 40 bar reasserted the two-stage ignition of DME. Dagaut and coauthors [16, 19] used a jet-stirred reactor (JSR) to study DME oxidation at pressures up to 10 atm. Dryer and coauthors [17, 18, 20, 21] explored DME oxidation in flow reactors and RCM's at pressures below 20 atm. Their results were interpreted in tense of a chemical kinetic model in [17]. Other shock-tube studies by Li et al. [23], Hu et al. [12], Tang et al. [11], and Burke et al. [23] reported ignition delays at pressures below 25 bar. Ignition delays are valuable as benchmarks in studying combustion, but details of the oxidation chemistry cannot be drawn from them. Species profiles upon ignition from flow reactors can offer additional detailed insight into the involved chemistry.

Despite its importance, DME interactions with natural gas components were rarely characterized. Amano and Dryer [9] reported flow-reactor measurements of CH₄/ DME oxidation at 10–18 atm and 800–1060 K. Burke et al. [23] measured ignition delays of CH₄/ DME mixtures over 10–30 atm and 600–1400 K. Other studies of DME addition to natural gas components [10–13] were limited to temperatures above 1000 K. Extending data to high pressure and intermediate temperature is beneficial in understanding CH₄/DME interactions.

In this work, we present results of DME pyrolysis and oxidation tests at 50 bar and 450–900 K as well as results of tests on methane doped with DME at 100 bar pressure and 450–900 K, all experiments conducted in a flow reactor. In addition to stoichiometric conditions, oxidation data are collected at strongly reducing (Φ∼20)

---

and very oxidizing conditions (Φ~0.05). Furthermore, a detailed chemical kinetic model is evaluated against the present data.

Experimental approach

The experimental setup was a laboratory-scale high-pressure laminar-flow reactor designed to approximate plug flow [24]. The setup was described in detail elsewhere [24] and only a brief description is provided here. The system was used here to study the oxidation chemistry of DME as well as its mixtures with methane. DME experiments were conducted at 50 bar pressure and with a constant flow rate of 4.53 NL/min (STP; 1 atm and 273.15 K). The oxidation of methane doped by DME was studied at 100 bar and at a flow rate of 3.23 NL/min (STP). The reactions took place in a tubular quartz reactor (inner diameter of 8 mm) to minimize the effects of surface reactions. The quartz reactor was enclosed in a stainless steel tube that acted as a pressure shell. The system was pressurized from the feed gas cylinders and the pressure fluctuations of the reactor were limited to ±0.2%. The steel tube was placed in a tube oven with three individually controlled electrical heating elements that produced an isothermal reaction zone (±6 K) of ~37–41 cm in the middle of the reactor. A moving thermocouple was used to measure the temperature profile inside the pressure shell at the external surface of the quartz tube after stabilizing the system. The gases were mixed at ambient temperature well before entering the reactor so a complete mixing was expected before the reactor. All gases used in the present experiments were high purity gases or mixtures with certified concentrations (±2% uncertainty). The total flow rate was measured by a bubble flow meter downstream of the reactor. Using a quartz tube and conducting experiments at high pressures were expected to minimize the contribution from heterogeneous reactions at the reactor wall.

Downstream of the reactor, the system pressure was reduced to atmospheric level prior to product analysis, which was conducted by an on-line 6890N Agilent Gas Chromatograph (GCTCD/ FID from Agilent Technologies) calibrated according to the procedure in [25]. The GC allowed detection of O_2, CO, CO_2, CH_4, C_2H_4 and C_2H_6 with estimated uncertainties around 5%. A larger uncertainty was estimated for measuring methanol and formaldehyde.

Figure 1 shows the measured temperature profiles of nitrogen flow with flow rate and pressure corresponding to the DME experiments. Over this work, it was found that considering only the isothermal zone of the reactor in interpreting and simulating the data can be misleading, due to the high reactivity of DME at the low temperatures at the heating zone of the reactor. Therefore, a plug flow approximation with constrained temperature according to the measured profiles was used for modeling in Chemkin [26].
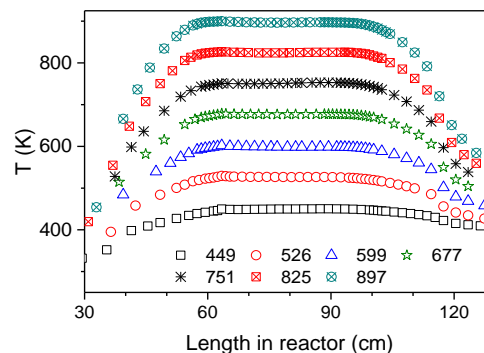

Figure 1: Measured temperature profiles across the reaction zone. The flow was pure nitrogen with a flow rate of 4.53 NL/min at a pressure of 50 bar.

Chemical Kinetic Models

The present reaction scheme consists of $H_2/C_1/C_2$/alcohols submodels developed in [25, 27–30]. The DME submodel is taken from Zhao et al. [17] with some modifications. The oxidation subset for formic acid is taken from a recent study by Marshall and Glarborg [31].

Results and Discussion

Species profiles from DME pyrolysis and oxidation in the flow reactor at intermediate temperatures (450–900 K) and high pressure (50 bar) are presented in this section. Later, the results of the oxidation of methane doped by DME over 450–900 K and at 100 bar are presented and compared with the neat methane oxidation in [25].

Neat DME experiments in the flow reactor

Figure 2 gives results from DME pyrolysis experiments. The DME dissociation starts around 825 K, where a trace amount of methane is detected. At higher temperatures, CH_2O and CO are detected too. Carbon is balanced well within ±3%. Although the model overpredicts slightly the conversion of DME at high temperatures, it predicts the experimentally observed changes in the concentrations fairly well.

Under reducing conditions (Φ=20, figure 3), the DME consumption starts around 525 K and CO is detected above 550 K. Between 575 K and 675 K, the concentration of DME remains almost constant, an indication of the expected NTC behavior. The NTC is more pronounced in the oxygen profile in which two inflection points characterizing the NTC zone can be identified at 575 and 625 K. Between these points, the oxygen fraction increases with increasing temperature. DME oxidation resumes at higher temperatures and oxygen is completely consumed. Below 725 K, the major detected product is formaldehyde, but above 725 K, CO and CH_4 become the major products while formaldehyde is still non-negligible. Trace amounts of ethene and ethane are also measured above 700 K.

The model predicts well the complicated non-monotonic changes in species fraction against temperature. The concentrations of CH_4, CO, and C_2H_6

2

are also well reproduced by the model. Although formaldehyde fraction is overpredicted, the trend of its change is reasonably predicted by the model.
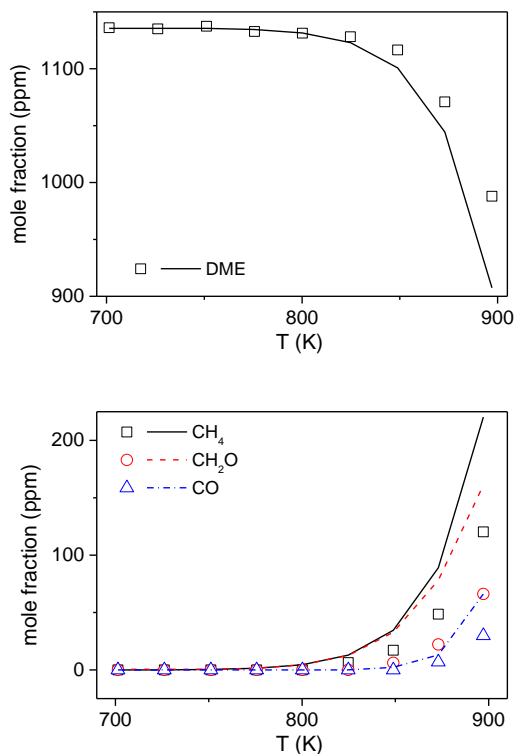

Figure 2: Results of DME pyrolysis experiments (1136 ppm of DME in N_2) at 50 bar

Balancing carbon in the fuel-rich experiments reveals 12% carbon loss in the worst case. According to the simulations, formic acid (HOCHO) and methyl formate (CH_3OCHO) should be formed in trace amounts under current conditions, but our measuring facility does not allow us to quantify these components. Adopting the concentrations of formic acid and methyl formate from the model, the carbon balance is improved to 10%.

The NTC behavior of DME is more pronounced under stoichiometric conditions (figure 4). The onset of DME reaction is found around 525 K, where trace amounts of CO and CO_2 are detected. The first inflection point can be identified at 575 K; above this point the fraction of reactants increases as temperature is raised. This NTC trend continues until 650 K, the second inflection point. Above 650 K, the DME consumption is accelerated as temperature rises. DME disappears completely above 775 K. In contrast, the oxygen consumption is confined to maximum 60%, likely due to the slow oxidation of CO at such temperatures. The inflection points can also be identified in the CO and CO_2 profiles. Within these points, product formation is retarded. An interesting trend in CO_2 fraction is seen at 800–900 K, where it falls but soon rises by elevating temperature. Methane increases monotonically with temperature and is formed

in trace amounts above 725 K. Formaldehyde peaks around 700 K and disappears above 750 K.

The model predicts well the onset of reaction, the inflection points, and the fractions of DME, O_2, CO, and CH_4. However, it slightly overpredicts formaldehyde, and underpredicts CO_2 in the NTC zone. The simulations show that methyl formate (CH_3OCHO) and formic acid (HOCHO) are produced up to 40 and 84 ppm, respectively. Adopting their fractions from the model, carbon is balanced within ±6%.

For the fuel-lean mixture (Φ=0.04), oxidation starts around 525 K. The NTC inflection points can be positioned at 575 and 675 K. Between these points, DME fraction remains almost constant but it disappears completely above 700 K. A similar plateau can be seen in the CO and CO_2 profiles over the same temperatures. Interestingly, CO fraction is almost independent of temperature and it stays around 90 ppm over 575–900 K.
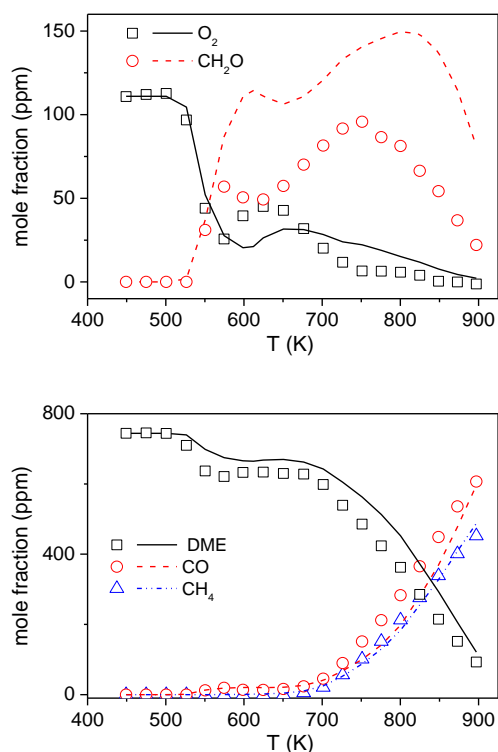

Figure 3: Results of DME reducing experiments at 50 bar (744/ 111 ppm of DME/ O_2 in N_2, Φ =20.2)

The model predicts well the onset of oxidation, the shapes of the profiles, and the fractions of the major components. However, it slightly underpredicts CO_2 formation at NTC zone, similar to the stoichiometric conditions. The model predicts the maximum formation of methyl formate and formic acid in considerable amounts of 30 and 86 ppm, respectively. Adopting these concentrations from the model, the carbon loss in the experiments is less than 14%.

In the DME oxidization experiments, the onset temperature of DME reaction is around 525 K, independent of the fuel-air equivalence ratio. The

inflection points corresponding to the NTC regime are slightly sensitive to changes in the stoichiometry, but generally NTC zone includes temperatures of 575–625 K. These results are in line with the results of earlier jest-stirred reactor [16] and flow reactor [18, 32] experiments where DME ignition was reported around 525–550 K and the NTC zone included temperatures of 600–700 K, despite differences in their initial reactants concentrations and pressure.
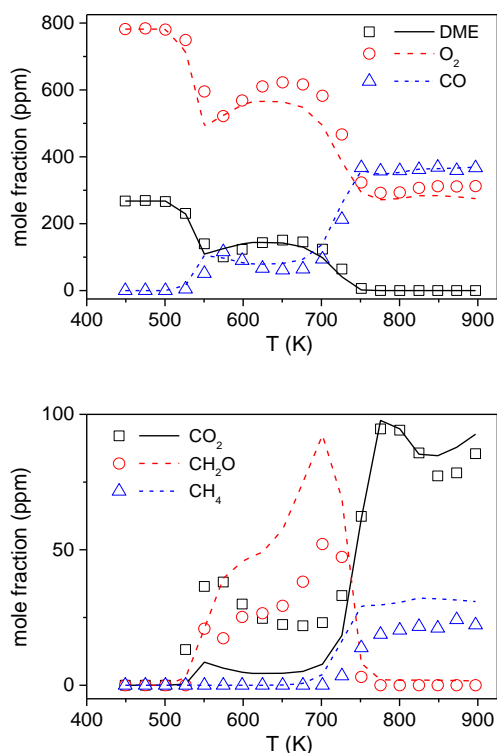
studies can help a better evaluation of models. Moreover, the GC is not configured for quantifying C_3 components, and the model also does not include C_3 subset. Therefore, it is likely that the observed carbon loss in the experiments is partly due to the formation of C_3 components.

Methane doped with DME experiments

The effect of doping methane with small amounts of DME on the fuel oxidation is investigated in the flow reactor at a pressure of 100 bar. Neat methane oxidation data are taken from [25] and are shown here for comparison.

Figure 4: Results of DME experiments under stoichiometric conditions and at 50 bar (268 /782 ppm of DME /O_2 in N_2, $\Phi=1.0$).
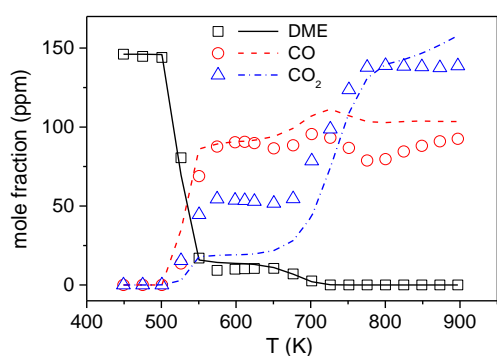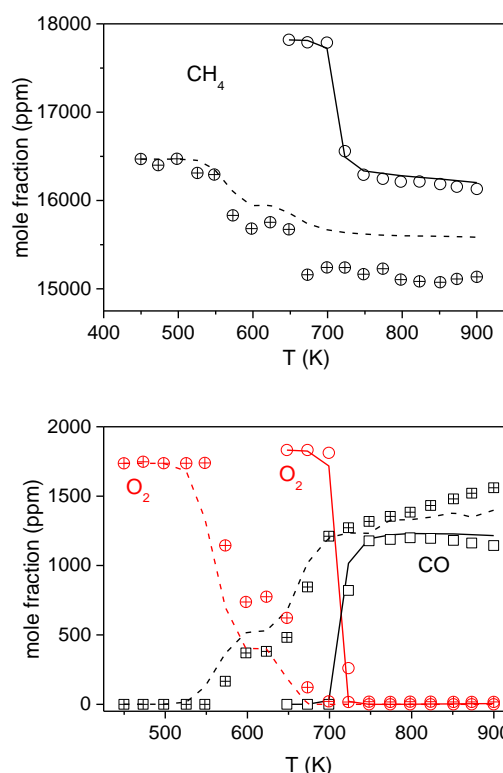

Figure 5: Results of DME oxidizing experiments at 50 bar (146 /10774 ppm of DME /O_2 in N_2, $\Phi=0.04$).

As outlined earlier, the current experimental facility does not allow quantifying formic acid and methyl formate whereas the model predicts a considerable yield of them, especially under stoichiometric and oxidizing conditions. Measuring these components in future

Figure 6: Results of DME addition to methane under reducing conditions ($\Phi=19.5–20.0$) and at 100 bar. Open symbols/solid lines: the neat CH_4 experiment [25] with 1832/17819 ppm of O_2/CH_4; Crossed symbols/dashed lines: the doped experiment with 1736/ 16469 /530 ppm of O_2 /CH_4 /DME; all diluted in N_2.

Figure 6 presents the results of experiments under reducing conditions (Φ=19.5–20.0). Constraining the fuel-air equivalence ratio, DME is added to the mixture with the DME to CH_4 ratio of 3.2%. Such a small amount of DME has a striking effect, as the onset temperature of the fuel conversion shifts from ~725 K for the neat methane to ~575 K for the doped methane.

The effect of DME addition is not only on the ignition temperature, but also on the shapes of species profiles. For the neat DME experiment under reducing conditions, a plateau was observed in the DME profile over 575–675 K. Such a plateau now can be identified around 600–650 K for the doped experiments, not only in DME profile, but also in O_2 and CO profiles. It seems that the doped mixture inherits the two-stage ignition from DME. The first stage of ignition takes place around 575 K, a temperature higher than that of neat DME at 50 bar (525 K). The second one is around 675 K, a temperature lower than the ignition temperature of neat methane (725 K). The earlier ignition triggered by adding DME promotes the formation of CO_2 and CO at high temperatures. DME fraction fluctuated slightly ($\pm3\%$) before the ignition, but that is within the uncertainty range of our experiments.

Whereas the onset of reaction under reducing conditions is predicted accurately by the model for both neat DME and neat methane [25], the ignition of methane mixed with DME is predicted slightly premature. This results in the slight underpredictions of DME and oxygen over 550–700 K. However, the model accurately reproduces the changes observed experimentally in DME, O_2, and CO, profiles.

Under stoichiometric conditions (Φ=0.99–1.02), two sets of experiments are conducted with the DME to CH_4 ratios of 1.8% and 3.2%. For both cases, the DME conversion starts around 675 K, but there is no consumption of CH_4 and O_2 below 700–725 K (see figure 7). As neat methane ignites at 750 K, the addition of DME triggers methane oxidation at temperatures 25–50 K lower. The NTC behavior can be identified only in the DME profiles over 725–750 K. Apart from that, the species profiles show a monotonic sensitivity to temperature. The concentrations of the major products at high temperatures are not sensibly affected by DME addition.

The model predicts well the onset of methane conversion as well as the fractions of O_2, CH_4, CO, and CO_2, but it underestimates the ignition temperature of DME in both doped mixtures, i.e. 550–575 K instead of 650 K. This premature DME conversion affects the DME profiles at higher temperatures. Surprisingly, the predictions of methane and oxygen fractions have not been affected by the premature ignition of DME.

Neat DME ignites at 525 K (at 50 bar) for a wide range of stoichiometries, so it seems that methane suppresses the ignition of DME in the mixture. Methane might activate some chain-terminating paths in DME oxidation at low temperatures. Noting that the model was able to predict accurately the ignition of neat DME

and neat methane separately under a wide range of stoichiometries, it is likely that the potential inhibiting effect of methane on DME ignition is not well covered in the model.

Calculations show that heat released from DME oxidation in the doped mixture is negligible, so the promoting effect of DME addition is probably related to a dramatic growth in the concentrations of radicals.
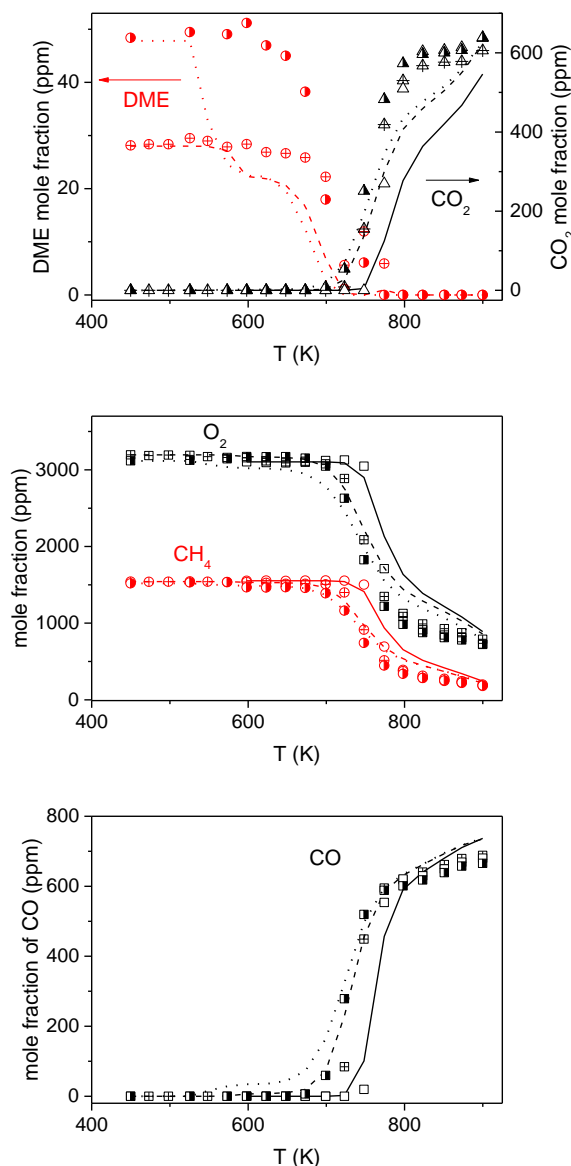

Figure 7: Results of DME addition to methane under stoichiometric conditions (Φ=0.99–1.02) and at 100 bar. Open symbols/solid lines: the neat CH_4 experiment [25] with 3104/1553 ppm of O_2/CH_4; Crossed symbols/dashed lines: the doped experiment (1.8%) with 3195 /1542 /28 ppm of O_2 /CH_4 /DME; Half-open symbols/dotted lines: the doped experiment (3.2%) with 3117 /1519 /48 ppm of O_2 /CH_4 /DME; all diluted in N_2.

Conclusion

The pyrolysis and oxidation of DME and its effect on methane oxidation as an additive have been

5

investigated in a flow reactor at high pressures and intermediate temperatures. It was found that DME pyrolysis started around 825 K at 50 bar pressure. The DME oxidation experiments at 50 bar gave the onset temperature of reaction at 525 K, independent of fuel-air equivalence ratio. Further experiments at 100 bar showed that by adding a small amount of DME to methane its ignition could effectively be accelerated. A model developed for DME/CH_4 oxidation was evaluated at a wide range of pressure, temperature, and stoichiometries. The model compared well with the data of neat DME oxidation from the flow reactor. Both onset temperature of reaction and the fractions of major components were reproduced fairly well by the model. The model could also outline the onset temperature of major reactions in CH_4/DME mixtures. Further work is needed to focus on interaction of DME/CH_4 in the model to address the premature DME depletion in CH_4/DME mixtures. The presented species profiles of DME and DME/CH_4 conversion extended the experimental benchmark for oxidation at high pressures and intermediate temperatures. Such benchmark are vital in validating chemical kinetic models developed for addressing problems in real conditions.

Acknowledgment

References

[1] International Energy Agency, Key world energy statistics, International Energy Agency, 2014.

[2] U.S. Energy Information Administration, International Energy Outlook 2013, EIA, Washington, 2013.

[3] D. Cipolat, Appl. Therm. Eng. 27 (2007) 2095 – 2103.

[4] C. Arcoumanis, C. Bae, R. Crookes, E. Kinoshita, Fuel 87 (2008) 1014 – 1030.

[5] G. Thomas, B. Feng, A. Veeraragavan, M. J. Cleary, N. Drinnan, Fuel Process. Technol. 119 (2014) 286–304.

[6] S. Sidhu, J. Graham, R. Striebich, Chemosphere 42 (2001) 681–690.

[7] L. Xinling, H. Zhen, Sci. Total Environ. 407 (2009) 2234 – 2244.

[8] M. C. Lee, S. B. Seo, J. H. Chung, Y. J. Joo, D. H. Ahn, Fuel 88 (2009) 657 – 662.

[9] T. Amano, F. L. Dryer, Symp. (Int.) Combust, [Proc.] 1 (1998) 397–404.

[10] Z. Chen, X. Qin, Y. Ju, Z. Zhao, M. Chaos, F. L. Dryer, Proc. Combust. Inst. 31 (2007) 1215 – 1222.

[11] C. Tang, L. Wei, J. Zhang, X. Man, Z. Huang, Energy Fuels 26 (2012) 6720–6728.

[12] E. Hu, Z. Zhang, L. Pan, J. Zhang, Z. Huang, Energy Fuels 27 (2013) 4007–4013.

[13] W. B. Lowry, Z. Serinyel, M. C. Krejci, H. J. Curran, G. Bourque, E. L. Petersen, Proc. Combust. Inst. 33 (2011) 929–937.

[14] J. Zhang, E. Hu, L. Pan, Z. Zhang, Z. Huang, Energy Fuels 27 (2013) 6247–6254.

[15] U. Pfahl, K. Fieweger, G. Adomeit, Symp. (Int.) Combust., [Proc.] 26 (1996) 781 – 789.

[16] P. Dagaut, C. Daly, J. M. Simmie, M. Cathonnet, Symp. (Int.) Combust., [Proc.] 27 (1998) 361 – 369.

[17] Z. Zhao, M. Chaos, A. Kazakov, F. L. Dryer, Int. J. Chem. Kinet. 40 (2008) 1–18.

[18] H. Curran, S. Fischer, F. Dryer, Int. J. Chem. Kinet. 32 (2000) 741–759.

[19] P. Dagaut, J.-C. Boettner, M. Cathonnet, Symp. (Int.) Combust., [Proc.] 26 (1996) 627– 632.

[20] S. L. Fischer, F. L. Dryer, H. J. Curran, Int. J. Chem. Kinet. 32 (2000) 713–740.

[21] G. Mittal, M. Chaos, C.-J. Sung, F. L. Dryer, Fuel Process. Technol. 89 (2008) 1244 –1254.

[22] Z. Li, W. Wang, Z. Huang, M. A. Oehlschlaeger, Energy Fuels 27 (2013) 2811–2817.

[23] U. Burke, K. P. Somers, P. OToole, C. M. Zinner, N. Marquet, G. Bourque, E. L.Petersen, W. K. Metcalfe, Z. Serinyel, H. J. Curran, Combust. Flame 162 (2015) 315 –330.

[24] C. L. Rasmussen, J. Hansen, P. Marshall, P. Glarborg, Int. J. Chem. Kinet. 40 (2008) 454–480.

[25] H. Hashemi, J. M. Christensen, S. Gersen, P. Glarborg, Ignition of methane at high pressure and medium temperatures: Measurements and kinetic modeling, *(in progress)* 2015.

[26] Reaction Design, CHEMKIN-PRO 15131, Reaction Design, San Diego, CA, USA, 2013.

[27] H. Hashemi, J. M. Christensen, S. Gersen, P. Glarborg, Proc. Combust. Inst. 35 (2015) 553 – 560

[28] H. Hashemi, J. M. Christensen, P. Glarborg, Ignition and oxidation properties of ethane at high pressure, *(in progress)* 2015.

[29] H. Hashemi, J.M. Christensen, P. Glarborg, Experimental and kinetic modeling study of ethanol combustion at high pressures and intermediate temperatures, *(in progress)* 2015.

[30] V. Aranda, J. M. Christensen, M. U. Alzueta, P. Glarborg, S. Gersen, Y. Gao, P. Marshall, Int. J. Chem. Kinet. 45 (2013) 283–294.

[31] P. Marshall, P. Glarborg, Proc. Combust. Inst. 35 (2015) 153–160.

[32] F. Herrmann, P. Owald, K. Kohse-Hinghaus, Proc. Combust. Inst. 34 (2013) 771 – 778.